Available online at www.sciencedirect.com
SCIENCE DIRECT®
ELSEVIER
Ultrasonics 42 (2004) 853–858
Ultrasonics
www.elsevier.com/locate/ultras

An improved automated ultrasonic NDE system by wavelet and neuron networks

Fairouz Bettayeb [a,*], Tarek Rachedi [b], Hamid Benbartaoui [b]

[a] CSC, Research Center on Welding and Control, Route de Dely Brahin, BP: 64, Chéraga, Algiers, Algeria
[b] USTHB, University of Science and Technology, Algeria

Abstract

Despite of the widespread and increasing use of digitized signals, the ultrasonic testing community has not realized yet the full potential of the electronic processing. The performance of an ultrasonic flaw detection method is evaluated by the success of distinguishing the flaw echoes from those scattered by microstructures. So, de-noising of ultrasonic signals is extremely important as to correctly identify smaller defects, because the probability of detection usually decreases as the defect size decreases, while the probability of false call does increase. In this paper, the wavelet transform has been successfully experimented to suppress noise and to enhance flaw location from ultrasonic signal, with a good defect localization. The obtained result is then directed to an automatic Artificial Neuronal Networks classification and learning algorithm of defects from *A*-scan data. Since there is some uncertainty connected with the testing technique, the system needs a numerical modelling. So, knowing the technical characteristics of the transducer, we can preview which are the defects that experimental inspection should find. Indeed, the system performs simulation of the ultrasonic wave propagation in the material, and gives a very helpful tool to get information and physical phenomena understanding, which can help to a suitable prediction of the service life of the component.

Keywords: Ultrasonic NDE; Signal analysis; Wavelet transform; Neuron networks

1. Introduction

In the case of the ultrasonic non-destructive characterization of materials, the reflections from discontinuities appear in the *A*-scan as abrupt time localized changes resulting in time varying spectral characteristics. Generally, when we want to describe a signal in time and frequency, the first natural position is the one which gives a sense to its spectral countenance. As, the ultrasonic signal is modulated to the transducer central frequency, the transient signal is commonly limited in time and in frequency. Indeed, the defect echo contains information dealing with the material and the discontinuity and often, the material microstructures generate echoes which are randomly distributed in time. These echoes are commonly defined as additional noise. The concept of filtering can be applied to describe the operations of any linear shift invariant system, signal analysis and filtering are often performed in the frequency domain, and signals and filter impulse response are decomposed into a sum of sinusoids, with varying frequencies, amplitudes and phases. The Fourier transform makes the temporal and frequential descriptions needful and insufficient. Insufficient, because even, these descriptions take all the information, the manner by which it's displayed, is rather far from the physical reality to be exploitable. These limitations have been overcome by the wavelet transform introduced to the signal processing community. Since, no signal can be simultaneously and arbitrary localized in time and frequency, the more concentrated one (i.e. gauss signal) must be interpreted as an elementary carrier signal of a minimum information. A wavelet has the characteristics of a pass band filter, and the wavelet transform has the properties of a continuous filter bank. Hence, because the energies of the ultrasonic signals are concentrated in a frequency band, all other frequencies are represented by very low amplitudes in the transform domain, and can be scattered without any loss of information. In this paper the Morlet function is adopted as the analyzing wavelet after an experimental study of the most suitable

* Corresponding author. Tel./fax: +213-21-361-850.
E-mail address: fairouz_bettayeb@e-mail.com (F. Bettayeb).

0041-624X/$ - see front matter © 2004 Elsevier B.V. All rights reserved.
doi:10.1016/j.ultras.2004.01.064

wavelet for the system. The enhancement of the flaw detection performance and noise suppression has been verified experimentally from several types of artificial and natural flaws.

2. Wavelet transform for ultrasonic NDE

The wavelet transform is the most recent technique for the processing of signals of which the spectral countenance is non-stationary. It is defined in term of basic function obtained by compression or dilatation and decay operations of the mother wavelet. In the wavelet transform, the signal spectrum is divided by an overlapping of pass band filters with constant relative bandwidth [1]. The continuous wavelet transform decomposes a temporal function $s(t)$ in a two-dimensional function of a scale 'a' and a delay 'τ' [1]. In the following formulas $h(t)$ is the mother wavelet, $h_{a\tau}(t)$ is the daughter wavelet and $C(a,\tau)$ is the correlation coefficient

$$C(a,\tau) = \int_{-\infty}^{+\infty} s(t) h_{a\tau}(t)\,\mathrm{d}t \tag{1}$$

$$h_{a\tau}(t) = \frac{h((t-\tau)/a)}{\sqrt{a}} \tag{2}$$

In the case of the ultrasonic signal, the analyzed waves have a piezoelectric transducer limited band. Therefore, the central frequency f_c of the mother wavelet is chosen so as it includes the central frequency of the ultrasonic impulse. Indeed, the optimal receipt filter for the detection of impulses swamped in Gauss noise, is a filter with an impulse response which has the same shape as the detected impulse, but it is inverted in time. This filter has the following frequency response:

$$H_{\mathrm{opt}}(f) = K\frac{Y^*(f)\mathrm{e}^{-\mathrm{j}\omega T}}{N(f)} \tag{3}$$

K: constant, $Y(f)$: spectrum of the impulse; $N(f)$: noise spectrum.

2.1. Analyzing wavelet and signal filtering process

In order to optimize the mother wavelet for our system, we have experimented with a number of analytical wavelets 44 plan and 35 volumetric defect signals. Table 1 displays the coefficients $C(a,\tau)$ which are the maximum amounts computed, after a successive passage of the defect signals through the filter banks. For the purpose of an easiest implementation, we have chosen from this table the Morlet function as the analyzed wavelet. Afterward, the process begins with the computing of the signal FFT by which we can adjust the nominal frequency of the transducer, followed by the coefficients wavelet transform computing. The filtering process developed in Eqs. (4) and (5), allows a significant de-noising inside the frequency band. The obtained result is converted to the time domain by the inverse wavelet calculation (see Fig. 1).

$$C_f(a,\tau) = 0 \quad \text{for } |C(a,\tau)| < \lambda \tag{4}$$

$$C_f(a,\tau) = \mathrm{sgn}[C(a,\tau)]\cdot(|C(a,\tau)| - \lambda) \quad \text{for } |C(a,\tau)| \geqslant \lambda \tag{5}$$

λ is the chosen threshold in the time scale representation. In the case of an automated ultrasonic inspection system, it is recommended to choose λ in the interval of 1.6 to double of the significant noise level (4–6 dB) [2].

The ultrasonic echo envelope, gives information on the time of flight of the wave in the material. The distance between the maximums, yields exactly the location of the defect or the material depth. Our system has given excellent results on the flaw location with an error about

Table 1
Some experiments for the ultrasonic mother wavelet choice

Defect signals	Mexican hat	Morlet	$Gauss_1$	$Gauss_2$	$Gauss_3$	$Gauss_4$	$Gauss_5$	$Gauss_6$	$Gauss_7$	$Gauss_8$
p14	0.14	**0.17**	0.12	0.14	0.15	0.15	0.16	0.16	**0.17**	**0.17**
p15	0.13	**0.16**	0.12	0.13	0.14	0.14	0.15	0.15	**0.16**	**0.16**
p16	0.15	**0.19**	0.14	0.15	0.16	0.17	0.18	0.18	**0.19**	**0.19**
p20	0.15	**0.19**	0.14	0.15	0.16	0.17	0.18	0.18	**0.19**	**0.19**
p21	0.16	**0.20**	0.15	0.16	0.18	0.18	0.19	0.19	**0.20**	**0.20**
p22	0.21	**0.27**	0.19	0.21	0.23	0.24	0.25	0.26	0.26	**0.27**
p25	0.16	**0.21**	0.14	0.16	0.17	0.19	0.18	0.20	0.20	**0.21**
p26	0.16	**0.21**	0.16	0.17	0.19	0.19	0.20	0.20	**0.21**	**0.21**
v29	0.13	**0.16**	0.12	0.13	0.14	0.14	0.15	0.15	**0.16**	**0.16**
v30	0.14	**0.17**	0.13	0.14	0.15	0.16	0.16	0.17	**0.17**	**0.17**
v31	0.15	0.18	0.14	0.15	0.17	0.17	0.18	0.18	**0.19**	0.18
v32	0.15	**0.18**	0.13	0.15	0.16	0.17	0.17	0.18	**0.18**	**0.18**
v33	0.18	**0.23**	0.17	0.18	0.20	0.21	0.22	0.22	**0.23**	**0.23**
v34	0.21	**0.26**	0.18	0.21	0.22	0.23	0.24	0.25	**0.26**	**0.26**

In bold, the maximum correlation coefficients '$C(a,\tau)$' between wavelets and defect signals. (p_i: planar; v_j: volumetric).

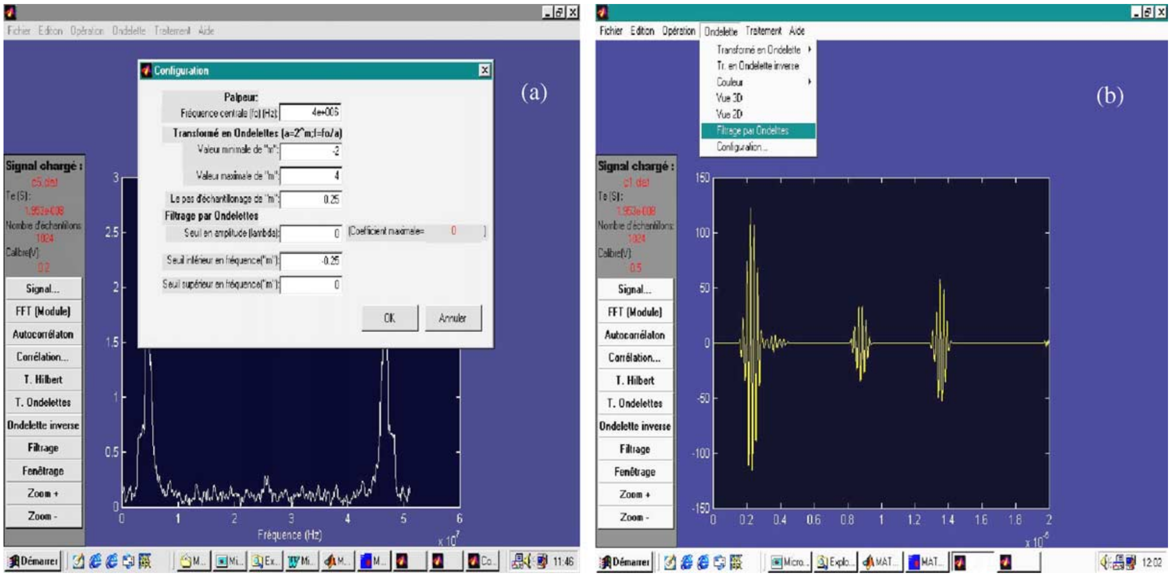

Fig. 1. (a) The detection interface, (b) the obtained filtered signal.

0.1 mm with the using of the Hilbert transform on the filtered signal.

2.2. Experiments

The experiments have been conducted with the following conditions:

- *Transducer 1*: $f_c = 6$ MHz, 10 mm diameter,
- *Transducer 2*: $f_c = 4$ MHz, $\theta = 45°$, 8×9 mm,
- *Transducer 3*: $f_c = 4$ MHz, $\theta = 60°$, 8×9 mm,
- *Transducer 4*: $f_c = 4$ MHz, $\theta = 70°$, 8×9 mm.
- *Piece 1*: steel material, 34 mm depth with artificial *circular* defects of 10, 7, 5, 3, 1 mm.
- *Piece 2*: steel material, 34 mm depth with artificial *cylindrical* defects of 10, 7, 5, 3, 1 mm.
- *Piece 3*: steel material, 17 mm depth with two artificial rectangular defects of 6 mm length.
- *Piece 4*: a welded steel material, 14 mm depth with lack of fusion and porosity defects.
- *Piece 5*: a welded steel material, 14 mm depth with group of porosity defect.

Figs. 2 and 3 display some results from the detection process developed below.

3. Ultrasonic neural network classifier

The material quality estimation depends on a large body of knowledge based on ultrasonic operator's competence and experience. In manual testing particularly, the identification of relevant from non-relevant indications as well as defect characterization, is highly examiner dependant. And, usually during the examination the operator is alone, depending only on his own observation of the signal features, such us echo shape, amplitude level, defect position within the geometry, rotation of the transducer around the defect location, etc. These parameters which, for some of them, no figure can be put, are combined by the operator in an implicit way to lead to the diagnosis. This signal shape recognition joined with heuristics rules, ensure a natural extension in the exploitation of the artificial neural networks 'Ann'. Choosing the architecture of a neural network for a particular problem usually requires some prior knowledge of the problem's complexity [3]. In this study, the 'Ann' classifier is trained to represent some decision between the two classes about planar and volumetric defects to be recognized. In Fig. 4 the input layer characterizes the envelop shape of the defect signal called the defect map, received from a numerical oscilloscope on 1024 samples filtered in a vectored representation. And the output layer is a Boolean representation of the two classes.

3.1. Defect recognition features

Drawing an automatic recognition of defects requires a powerful formalism. A detailed knowledge of the interaction between ultrasonic waves and defects, the propagation medium and the conditions in which ultrasonic investigations are curried out, are all elements of basic importance in defect recognition [4]. The strategy is to extract some parameters, enabling the featuring of the pulse echo envelope reflected from a defect on *A*-scan images obtained using a single transducer, about the maximum reflection transducer position and

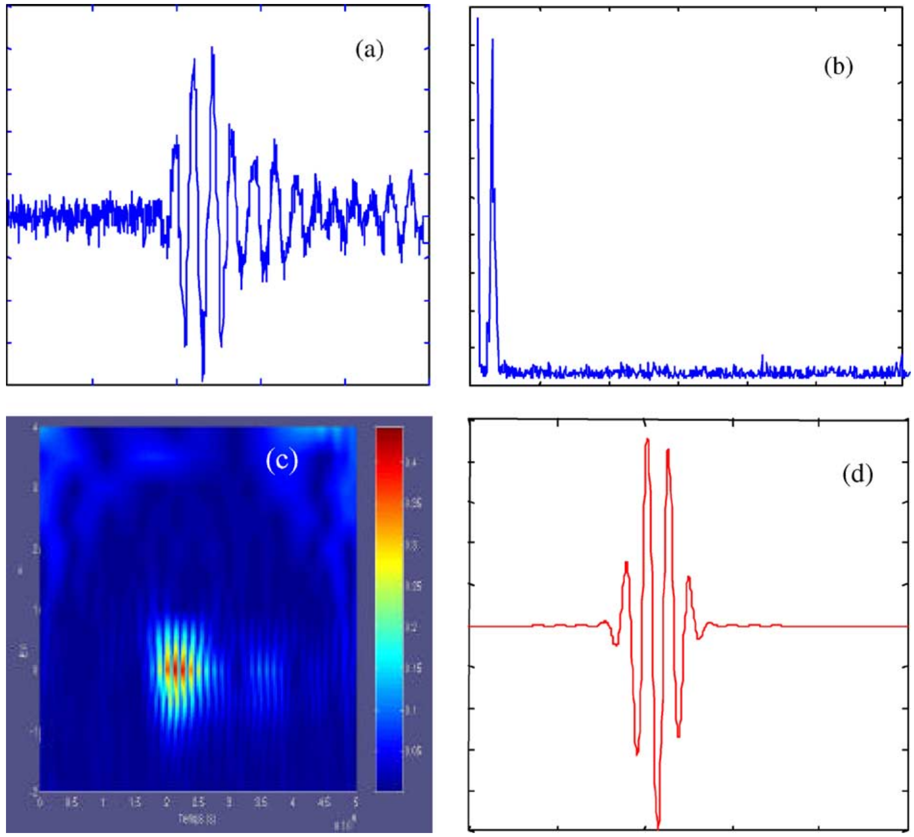

Fig. 2. (a) Group of porosity signal, (b) its FFT, (c) the defect wavelet, (d) the filtered signal.

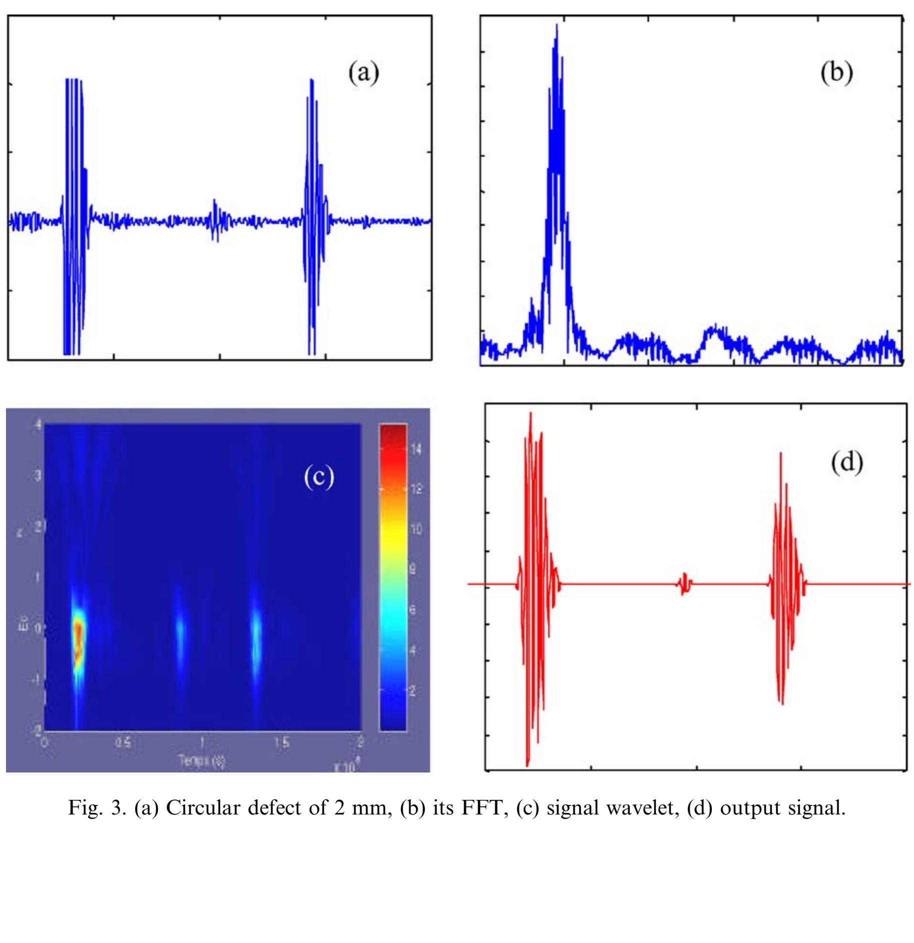

Fig. 3. (a) Circular defect of 2 mm, (b) its FFT, (c) signal wavelet, (d) output signal.

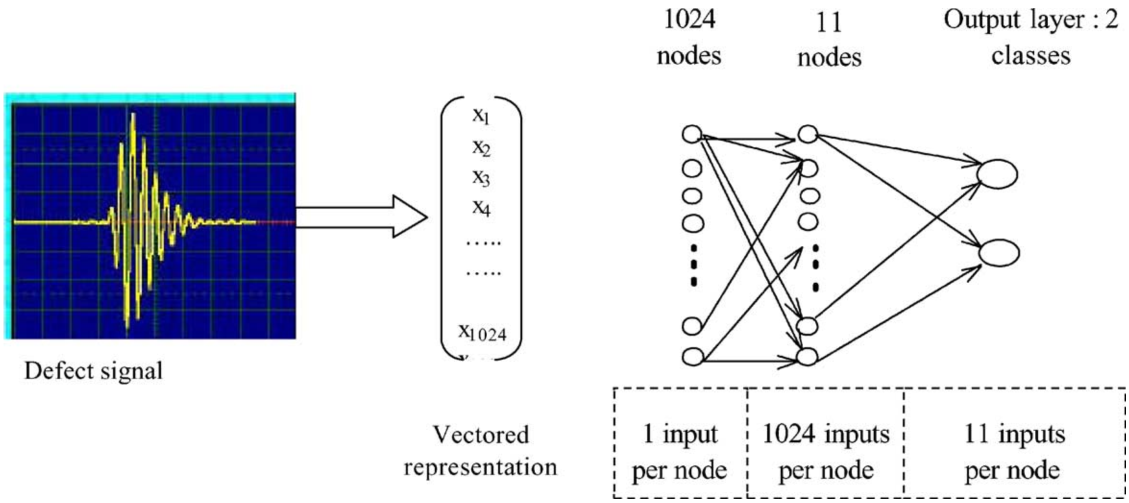

Fig. 4. Network architecture of the system.

Table 2
Defect recognition rules from manual testing

Defect type	Echo form	Echo form after transducer movement from the defect location		
		M^{vt} ∥ to the joint[a]	M^{vt} ⊥ to the joint [a]	Around the joint
Porosity	With jagged aspect	The echo disappears rapidly	The echo declines quickly	The echo is nearly constant
Porosity group	Set of small echoes with stiff fronts	The global echo persists, with mobility of the sub echoes position	Same conditions as ∥ movement	Same conditions as the other movements
Slag inclusion	Has an irregular front	The echo persists but its shape changes	The echo go away rapidly	The echo decreases gradually
Imperfect penetration	The echo is high with stiff front	The echo behavior subsists	As for ∥ movement	The echo disappears
Lack of fusion[b]	As for lack of penetration	Same conditions	Same conditions	Same conditions
Cracks	Superposition of high echoes, with stiff front	The echo persists	The echo persists	The echo reduces and raises without going out

[a] (∥: parallel, ⊥: perpendicular).
[b] The only difference is about the defect position.

the transducer-defect distance variation. Some of the knowledge rules for the most important defects are listed in Table 2.

3.2. Learning process

After initializing the network, the learning starts with applying the training vector to the network input. This vector is processed through the different layers. At the network's output the error between the actual and the desired output is measured. This error is afterward minimized by back propagating it through the network and by reconfiguring the neurons and their weight's matrices in the whole network. This is repeated for all training patterns until the algorithm converges to a small error. Since the back propagation algorithm requires differentiability along the network signal path, we adopt as a transfer function at each unit the 'Sigmoid' function [5] as follows:

$$F = 1/(1 + e^{-\sum ax+b}) \tag{6}$$

a: is the weight; x: is the input of the unit. b: is randomly selected in $[-0.5, 0.5]$ at start state and modified during training.

In order to evaluate the weights, they have to be trained from a random set of initial weights, using the training back propagation algorithm, with a minimizing process of the objective function (7) by a gradient descent procedure. This is done by the choice of the conventional mean squared error function 'MSE' [6].

$$E(x) = 1/2 \sum_{j=1,nl} (x_d - x_j)^2 \tag{7}$$

The performances of the system are displayed in Table 3.

Table 3
System performances

Defect classes	Recognition rate (%)	Reject rate (%)	Confusion rate (%)
Plan	95	0	5
Volumetric	100	0	0
Total	97.5	0	2.5

4. Conclusion

Since NDE is an "expert" oriented field, the ability of learning systems to offer a framework for emphasizing the manner in which decisions are made, and then to formalize the path by which they are reached, is exceptionally essential for automation purpose. In this paper we have worked on artificial flaws from steel plates, and on some natural defects from welds, for which the obtained signals are sampled on 1024 points. And for each defect location, we have taken several signals dealing with different transducer positions. The learning is performed on about 90 patterns. Future work concerns the search of an optimal configuration of the global network in which a sub net of each defect family will be included, so that to obtain a more categorical apprenticeship stage. However, for accuracy and effectiveness needs, our classification scheme has been accompanied by an ultrasonic 'level 2' IAEA certified inspector. On the other hand, in this study the achievement of ultrasonic signal de-noising, using wavelet analysis of ultrasonic echo waveform, has been verified experimentally. Hence, the wavelet transform seems to be a possible and powerful processing step of the whole automatic process of ultrasonic quality control.

References

[1] R.K. Young, Wavelet Theory and its Application, Academic publishers, 1993, Edition Kluwer.
[2] A. Abbate, J. Koay, J. Frankel, S.C. Schroeder, P. Das, IEEE Trans. Ultrason. Ferroelectr. Freq. Control 44 (1) (1997) 14–25.
[3] P.F. Whelan et al., IEEE Syst. Man Cybernet. 26 (5) (1996) 533–544.
[4] F. Bettayeb et al., in: 3rd International Conference on NDE in Relation to Structural Integrity for Nuclear and Pressurized Components Proceeding, Nov 2001, Seville.
[5] X. Yao, Y. Liu, IEEE Trans. Neural Networks 8 (3) (1997) 694–713.
[6] I.K. Sethi, IEEE Trans. Syst. Man Cybernet. 25 (8) (1995) 1243–1248.